

Critical wind speeds suggest wind could be an important disturbance agent in Amazonian forests

Chris J. Peterson^{1*}, Gabriel Henrique Pires de Mello Ribeiro², Robinson Negrón-Juárez³, Daniel Magnabosco Marra^{2,4,5}, Jeffrey Q. Chambers³, Niro Higuchi², Adriano Lima² and Jeffery B. Cannon⁶

¹Department of Plant Biology, University of Georgia, Athens, GA 30602, USA

²Brazil's National Institute for Amazonian Research, Manaus-AM 69060-97, Brazil

³Lawrence Berkeley National Laboratory, Climate Science Department, Berkeley, CA 94720, USA

⁴Biogeochemical Processes Department, Max-Planck-Institute for Biogeochemistry, Jena 07745, Germany

⁵Institute of Biology, University of Leipzig, Leipzig 04103, Germany

⁶Colorado State University, Colorado Forest Restoration Institute, Fort Collins, CO, USA

*Corresponding author. E-mail: chris@plantbio.uga.edu

Received 27 January 2018

Recent research in the central Amazon suggests that wind is a major agent of disturbance, however, a mechanistic understanding of how wind may lead to tree mortality in Amazonian forests remains unclear. Here we estimated wind speeds necessary to topple central Amazon trees by linking both static and dynamic versions of two wind speed estimation methods (four methods total) to field data on tree failure derived from a static winching study. Static versions of these methods assumed invariant wind characteristics as more trees failed, while dynamic versions updated tree spacing, leaf area index and wind profiles progressively after each tree failure. First, we used a profile method which estimates wind force on individual trees by segments. We calculated drag on each segment and converted drag into basal turning moment, and compared the summed turning moments to the critical turning moment measured in the winching study. Estimated critical wind speeds from the static profile method varied greatly, from 10.75 m s⁻¹ to >120.0 m s⁻¹ with a mean of 45.70 m s⁻¹. Critical wind speeds estimated with static approaches decreased with tree size but were not significantly different between two focal genera. Primary drivers of variation in critical wind speed were tree height and crown size. Second, we used the turning moment coefficient method of Hale, S.E., Gardiner, B., Peace, A., Nicoll, B., Taylor, P. and Pizzirani, S. 2015 Comparison and validation of three versions of a forest wind risk model. *Environ. Model. Softw.* **68**, 27–41. doi:10.1016/j.envsoft.2015.01.016.; the static version of this method yielded less-variable estimates, ranging from 18.98 to 52.01 m s⁻¹, with a mean of 30.88 m s⁻¹. Notably, the two static methods for estimating critical wind speeds differed in the trees they identified as having the highest and lowest critical wind speeds. Dynamic variants of the above two methods produced greatly reduced ranges in CWS estimates for our study trees, because after the early tree failures, remaining trees were subject to greater wind penetration into the stand and thus greater loading for a given above-canopy wind speed. CWS estimated with dynamic approaches differed significantly between the focal taxa. Nevertheless, both estimates suggest that wind speeds commonly observed during Amazon storms are sufficient to produce widespread tree damage and mortality.

Introduction

Classical views of lowland moist tropical forests considered that small gaps were a common and perhaps predominant form of disturbance, and consequently a primary determinant of numerous fundamental forest characteristics (Denslow, 1980; Brokaw, 1985; Whitmore, 1989). Prominent in such thinking was the idea that small gaps might drive size structure, species composition and maintenance of diversity via specialization of different species on different niches along a resource gradient from

the centre to periphery of gaps, or (equivalently) specialists on gaps of different sizes (Denslow, 1980). A variety of recent findings, however, have spurred rapidly growing recognition of the potential importance of larger wind disturbances in Amazonian forests (Nelson *et al.*, 1994; Negrón-Juárez *et al.*, 2010; Chambers *et al.*, 2013; Magnabosco Marra *et al.*, 2014, 2018; Rifai *et al.*, 2016; Araujo *et al.*, 2017; Negrón-Juárez *et al.*, 2018). Thus, it is vital that we develop a mechanistic understanding of the underlying processes driving large-scale wind disturbances (Johnson and Miyanishi, 2007). Indeed, while other types of

ecological disturbances such as fire are understood at the level of underlying mechanisms – e.g. the physics of combustion (Mitchell *et al.*, 2009) – knowledge of the mechanics of wind disturbance is scarce for most regions and unavailable for Amazon forests. One step in developing such an understanding would be to determine what storm intensities (i.e. wind speeds) and gust durations will cause treefall, that is, the critical wind speeds (CWS); while such estimates are available for cool-temperate plantations and unmanaged boreal forests (e.g. Ancelin *et al.*, 2004; Achim *et al.*, 2005; Peltola *et al.*, 1999; Hale *et al.*, 2015; Kamimura *et al.*, 2016, reviewed in Mitchell and Ruel, 2015), they have not been attempted for highly diverse tropical forests. Given the growing understanding of the importance of wind disturbance in tropical forests, it would be timely to develop such estimates for Amazonian tree species.

Critical wind speeds (CWS) can be compared to weather records to determine how frequently such winds are experienced in particular locations (although time of measurements and location of meteorological stations together probably lead to underestimation of peak velocities). Such knowledge would provide insights into spatial or temporal variation in disturbance rates or magnitudes: if taxa differ substantially in vulnerability, then changes in species composition may explain variation in disturbance solely on the basis of the vegetation, independent of the weather. Therefore, we present estimates of the critical wind speeds for mature central Amazon trees, with a focus on *Scleronema micranthum* (Ducke) Ducke (MALVACEAE) and *Eschweilera* spp. (LECYTHIDACEAE), both dominant taxa in the central Amazon, but also including several other species; this is the first attempt, to our knowledge, at such estimates for tropical moist forests. We initially employ two static approaches, which consider tree-failure on an individual-tree basis without varying wind characteristics as more trees fail; the two approaches are based on the tree stability models GALES (Gardiner *et al.*, 2008) and HWIND (Peltola *et al.*, 1999); most of the existing estimates of critical wind speed are based on some variant of these two models, although a few studies employ other approaches (e.g. finite element modelling, e.g. Ancelin *et al.*, 2004; Ciftci *et al.*, 2014). Subsequently, we extend these analyses to an iterative, dynamic approach that explicitly considers the sequence of tree failure and changing wind conditions as tree density decreases. Dynamic approaches should be superior to static approaches when damage is severe or complete, because the greater turbulence and wind penetration into the stand once failure of one or a few trees creates gaps (Cremer *et al.*, 1982; Mitchell, 2013), will by definition change the wind loading on the remaining trees. Several authors (e.g. Byrne and Mitchell, 2013; Dupont *et al.*, 2015) have pointed out that the dynamics of damage propagation may be such that ignoring propagation could bias CWS estimates and therefore damage levels.

Secondarily, static models of tree failure that estimate CWS on a tree-by-tree basis allow examination of whether particular tree attributes such as branching architecture, DBH, or crown size (area and volume) influence the variation in critical wind speed among individuals and across species. Such analyses will illuminate existing phenomenological studies, such as recent findings showing that there is differential damage among species (Magnabosco Marra *et al.*, 2014; Rifai *et al.*, 2016), which in turn promotes tree diversity (Magnabosco Marra *et al.*, 2014)

and has a decadal effect on patterns of biomass and functional composition (Magnabosco Marra *et al.*, 2018). Here we explore factors that drive variation among individuals in static estimates of critical wind speed, and test for consistent differences between the two most common genera in our data set. This work is an extension of recent findings in Ribeiro *et al.* (2016), who reported results of static winching tests that quantified the critical turning moment at the base of the tree for several species, although only two had sufficient sample size for statistical comparison.

Study site and methods

To estimate critical wind speeds, we utilize the critical turning moments and tree dimensions of 60 Amazon forest trees, reported in Ribeiro *et al.* (2016). Those authors followed established protocols for static winching, summarized in Nicoll *et al.*, (2006) and Peltola (2006). The study area was the Tropical Silviculture Experimental Station (EEST, per its acronym in Portuguese) located at 2.45°–2.66°S, 60.02°–60.32°W, 53 km north of the city of Manaus, Amazonas State, Brazil. The EEST covers 21,000 ha, dominated by old-growth forest (Andrade and Higuchi, 2009) where landforms include plateaus (90–105 m above sea level, asl) and small valleys (45–55 m asl) (Ferraz *et al.*, 1998; Renno *et al.*, 2008). Soils on the plateaus are generally of a clay texture, soils from the upper slopes are sandy clays, soils on the lower slopes are loamy sands and soils in the valleys are sand dominated (Ferraz *et al.*, 1998). Soil texture, organic matter content, soil moisture, soil pH and soil C and N concentrations vary significantly with elevation along topographic gradients in the Central Amazon (Luizao *et al.*, 2004). The forest is characterized by high diversity of tree species (Higuchi *et al.*, 1997; Saito *et al.*, 2003; Carneiro *et al.*, 2005) with a mean canopy height of ~30 m with the tallest trees exceeding 40 m (Lima *et al.*, 2007). Among the most common species of the study area are *Eschweilera coriacea* (DC.) S.A. Mori (mata matá) and *Scleronema micranthum* (cardeiro); *Eschweilera* spp. in the aggregate make up a hyperdominant genus in the area (Ribeiro *et al.*, 1999; Higuchi *et al.*, 2004; Vieira *et al.*, 2004; Carneiro *et al.*, 2005). The mean density of stems above 10 cm DBH (diameter at breast height) is 584.3 ± 25.9 trees ha⁻¹ (da Silva *et al.*, 2002; Vieira *et al.*, 2004). Our study area is characterized by a mean annual temperature of 27°C and mean annual rainfall of 2365 mm with the dry season (rainfall <100 mm month⁻¹, (Sombroek, 2001)) falling between July and September (Negrón-Juárez *et al.*, 2017).

In our previous winching study, 60 trees were chosen such that 20 each represented the two most abundant taxa (across topographic positions such as plateaus and valleys) in the area (*Scleronema micranthum* (we only sampled one species) and *Eschweilera* spp (various species)), and 20 represented a mixture of other species (Ribeiro *et al.*, 2016). All trees were pulled with a hand winch and cable system identical to that used in Cannon *et al.* (2015), except that no pulley block was used. Two inclinometers, placed at 1.5 m and at the base of the crown, recorded inclination of the winched tree, and were synchronized with a load cell installed in-line in the cabling system. Winched trees ranged in diameter at breast height (DBH) from 19.1 cm to 41 cm (Table 2). A variety of biometric parameters were

Table 1 Parameters, values and units used in calculation of wind profiles, profile estimates of CWS and TMC estimates of CWS.

Symbol	Parameter name	Value	Units	Comments
<i>Used in calculating forest wind profile</i>				
\bar{u}_h	Wind speed at mean canopy height (30 m)	Varies	m s^{-1}	From de Santana et al. (2017)
μ	Fitted constant, wind profile	1.012	None	From de Santana et al. (2017)
β	Fitted constant, wind profile	0.1	None	From de Santana et al. (2017)
LAI	Leaf area index	6.7	None	From Filho et al. (2005)
z	Height above ground	Varies	m	From de Santana et al. (2017)
z_{ip}	Height of inflection point	30.0	m	From de Santana et al. (2017)
<i>Used in calculating open surroundings wind profile</i>				
U_0	Friction velocity	Varies	m s^{-1}	From Peltola (2006)
k	von Karman's constant	0.4	None	From Peltola (2006)
Z_0	Roughness length	0.05	m	From Peltola (2006)
<i>Used in profile estimates of CWS</i>				
ρ	Air density	1.12	kg m^{-3}	From Peltola and Kellomaki (1993)
C_d	Drag coefficient	Varies	None	From Peltola and Kellomaki (1993)
$A(z)$	Area of a vertical segment of crown or trunk	Varies	m^2	From Peltola and Kellomaki (1993)
$U(z)$	Wind velocity at height z	Varies	m s^{-1}	From Peltola and Kellomaki (1993)
D	Drag on a vertical segment	Varies	N	From Peltola and Kellomaki (1993)
b_1	Fitted constant, trunk taper	-2.5116	None	From Martin (1981)
b_2	Fitted constant, trunk taper	1.1587	None	From Martin (1981)
g	Acceleration due to gravity	9.82	m s^{-2}	From Peltola and Kellomaki (1993)
<i>Used in TMC estimates of CWS</i>				
h	Tree height	Varies	m	From Hale et al. (2015)
dbh	Tree diameter at 1.3 m	Varies	m	From Hale et al. (2015)
d_0	Tree basal diameter	Varies	m	From Hale et al. (2015)
h	Tree height	Varies	m	From Hale et al. (2015)
MOR	Modulus of rupture	Varies	MPa	From Hale et al. (2015)
f_{knot}	Knot factor	0.9	None	From Hale et al. (2015)
C_{reg}	Winching regression coeff.	207.19	Nm kg^{-1}	From Hale et al. (2015)
SW	Stem weight	Varies	kg	From Hale et al. (2015)
TMC_{ratio}	Turning moment coefficient ratio	Varies	None	From Hale et al. (2015)

measured manually on winched trees including DBH (cm), total tree height (m) measured after winching, height of crown base (in m; and thus by subtraction, crown depth) and stem mass (kg) (Table 1). Critical turning moments (M_{crit} , Nm) were calculated for the base of each winched tree. See [Ribeiro et al. \(2016\)](#) for details on calculation of critical turning moment.

To calculate crown area for each tree, after it was down, distance was measured from the centre of the trunk at the base of the crown, to the ends of branches in a series of locations moving anti-clockwise and in a plane parallel to the ground (using a True pulse 200X rangefinder; Laser Technology, Centennial, Colorado, USA); area was calculated from these measures by entering the azimuth and distance of each point from the base of the crown into a GIS software package and using the software to calculate the area of the polygon thus defined. This results in an area of a plane from bottom to top through the crown and which was oriented vertically when the tree was standing; the result is the two-dimensional area and it is assumed that this is not a biased measure of crown area. Note that throughout this manuscript, 'crown area' refers to the sail area or vertical profile in a standing tree (also sometimes called 'silhouette area'; it is the maximum vertical cross-sectional area).

Estimation of critical wind speeds

Background and general approach

The majority of estimates of critical wind speed employ similar approaches in the sense that (1) observed critical turning moments are measured, usually based on static winching; (2) wind load on trees is estimated on the basis of tree dimensions for many increments of wind speed; (3) the estimated wind load at various wind speeds is converted to a turning moment at the trunk base; and (4) the predicted basal turning moments are compared to the observed critical turning moment to infer the critical wind speed. The static winching methodology is quite consistent across studies ([Nicoll et al., 2006](#); [Peltola, 2006](#)), but there is greater variety in how wind loads are estimated. We used two static and two dynamic approaches; one each derived from the most prominent tree wind risk models GALEs ([Gardiner et al., 2008](#)) and HWIND ([Peltola et al., 1993, 1999](#)). Their primary difference is how forces on the trees are calculated. The roughness method used in GALEs estimates shear stress (total drag per unit area) imposed on the stand canopy by the wind, and then partitions this among the trees based on average distances between trees, thus estimating mean wind load on the

Table 2 Characteristics of study trees.

Tree	Species	DBH (cm)	Ht (m)	Crown Area (m ²)	Crown depth (m)	Critical Turn. Mom. (kNm)	Static CWS		Dynamic CWS	
							Profile method (m s ⁻¹)	TMC method (m s ⁻¹)	Profile method (m s ⁻¹)	TMC method (m s ⁻¹)
1	SCMI*	34.6	27.9	31.2	11.8	260.5	40.75	36.82	23.25	26.03
2	SCMI	31.6	26.1	23.0	10.6	197.3	55.50	37.51	24.50	26.09
3	SCMI	27.6	25.7	13.5	8.3	131.8	55.50	36.14	24.25	26.67
4	SCMI	29.8	26.8	28.9	9.5	195.8	37.50	34.16	22.75	27.02
5	SCMI	24.5	20.6	15.8	5.6	133.7	104.75	34.18	28.50	26.76
6	SCMI	20.0	21.0	17.4	9.7	132.7	118.00	29.52	30.75	25.40
7	SCMI	38.8	30.5	35.8	13.3	322.0	30.75	34.44	23.00	26.38
8	SCMI	35.0	23.9	21.2	10.6	260.8	95.75	39.90	31.50	25.66
9	SCMI	38.1	31.3	24.7	12.4	247.9	27.00	30.35	22.75	25.93
10	SCMI	19.5	22.1	37.4	8.9	63.0	27.00	25.40	20.00	23.78
11	SCMI	23.4	25.1	11.6	9.4	72.1	47.75	26.59	22.75	23.96
12	SCMI	25.2	24.3	13.4	12.9	172.8	106.25	29.16	33.25	25.44
13	SCMI	36.9	28.1	39.0	12.1	244.4	31.50	34.05	22.00	27.46
14	SCMI	23.1	25.2	17.2	9.3	106.4	40.75	29.44	22.50	25.52
15	SCMI	21.8	25.1	19.2	8.2	133.1	45.00	25.90	22.75	24.00
16	SCMI	19.0	22.3	NA	8.6	72.9	45.25	27.28	22.50	24.42
17	SCMI	36.3	30.2	31.5	12.5	271.7	29.25	33.98	22.75	27.65
18	SCMI	38.8	27.7	35.1	12.7	372.4	53.25	30.67	27.00	26.01
19	SCMI	20.9	21.7	19.5	8.2	59.3	41.25	32.78	22.00	27.14
20	SCMI	38.2	29.2	41.3	10.2	276.0	26.00	33.65	21.00	27.62
21	ESSP	31.1	24.4	73.3	14.7	223.6	41.00	22.41	22.25	22.08
22	ESSP	24.9	24.1	26.5	8.9	114.3	39.25	38.38	22.00	25.24
23	ESSP	30.2	25.2	33.7	10.0	206.5	46.25	52.01	22.75	28.69
24	ESSP	19.6	23.1	31.2	8.8	74.8	29.25	34.39	20.25	26.63
25	ESSP	29.2	26.4	44.0	13.6	211.1	39.75	24.84	22.50	23.50
26	ESSP	39.5	28.9	85.1	16.6	295.1	23.25	45.97	19.75	28.10
27	ESSP	24.7	23.0	84.0	11.8	196.7	34.50	24.13	21.75	23.37
28	ESSP	22.1	18.1	15.3	6.3	87.4	117.25	38.06	27.50	26.02
29	ESSP	22.4	18.9	35.7	11.3	61.4	48.00	22.01	22.50	21.77
30	ESSP	37.0	30.7	64.6	11.2	285.2	14.00	25.83	13.50	24.06
31	ESSP	28.1	23.4	63.1	15.5	202.2	51.00	42.79	22.75	26.87
32	ESSP	25.5	21.4	37.0	15.1	87.0	50.50	19.44	22.50	19.46
33	ESSP	20.5	22.9	29.1	11.9	87.2	36.75	32.38	21.75	27.03
34	ESSP	27.7	25.5	68.0	13.5	291.4	42.75	23.26	22.50	22.81
35	ESSP	24.3	21.5	23.0	8.0	108.5	60.50	36.21	22.75	26.37
36	ESSP	28.4	27.7	71.3	13.0	250.8	22.75	35.12	19.75	26.59
37	ESSP	23.9	24.4	40.9	11.7	195.0	45.25	34.10	22.50	27.24
38	ESSP	20.1	21.0	26.4	7.0	103.7	49.75	35.69	22.50	26.69
39	ESSP	36.5	23.5	29.7	10.2	201.4	67.25	23.91	24.50	23.26
40	ESSP	40.7	27.8	20.2	13.8	369.8	75.50	24.42	34.50	23.43
41	RIGU	36.5	20.2	30.0	11.2	108.8	73.00	19.71	22.75	19.66
42	INLA	31.9	28.4	40.9	12.1	168.4	22.50	36.59	19.50	26.26
43	DIMA	26.0	29.5	86.7	11.2	219.9	10.75	28.35	10.75	25.23
44	LEGR	41.1	28.3	42.1	11.0	346.1	38.25	46.10	23.00	27.36
45	ESTE	27.1	23.8	21.4	8.2	209.8	79.75	26.13	27.25	23.81
46	ANUN	28.7	25.4	20.9	8.5	124.3	38.00	29.00	22.25	25.48
47	BOMU	26.4	25.1	66.5	13.5	160.9	27.75	28.58	20.00	25.27
48	POCA	20.0	25.0	20.2	8.0	68.6	25.75	26.36	19.75	23.89
49	JACO	25.4	28.1	6.3	5.2	64.7	26.25	18.98	21.25	18.98
50	ESCO	27.6	25.3	41.2	9.3	111.8	23.50	25.17	19.50	23.69
51	IRJU	27.8	26.6	40.3	10.9	107.3	20.75	30.85	18.25	25.96

Continued

Table 2 *Continued*

Tree	Species	DBH (cm)	Ht (m)	Crown Area (m ²)	Crown depth (m)	Critical Turn. Mom. (kNm)	Static CWS		Dynamic CWS	
							Profile method (m s ⁻¹)	TMC method (m s ⁻¹)	Profile method (m s ⁻¹)	TMC method (m s ⁻¹)
52	APTU	26.3	24.8	18.7	7.0	133.9	49.75	24.25	23.00	23.38
53	VIPA	33.0	25.6	28.2	8.3	133.1	32.75	20.79	21.75	20.65
54	CHKA	27.9	28.1	41.1	10.7	111.8	15.75	24.66	14.50	23.43
55	<u>RUSP</u>	24.9	27.1	22.4	9.8	104.3	24.50	25.98	19.75	23.94
56	MISP	30.5	30.6	43.0	12.1	197.9	16.25	24.50	15.00	23.39
57	EPGL	38.0	22.0	24.1	9.1	299.9	>120.0	26.09	34.50	23.91
58	<u>OUDI</u>	22.2	21.3	27.7	9.3	60.2	38.00	38.16	21.75	25.60
59	<u>SIAM</u>	21.6	24.4	14.5	8.6	32.3	22.75	23.50	19.25	22.95
60	<u>EPGL</u>	35.3	25.0	41.0	11.9	127.5	33.00	51.57	21.50	29.59

Maximum and minimum in each column are in bold. CWS = critical wind speed at mean canopy height (i.e. 30 m). TMC = turning moment coefficient. Trees with underlined taxon acronym experienced trunk breakage; the remaining trees uprooted.

*Asterisk explains the acronyms used in table, and links to first row of table data.

SCMI – *Scleronema micranthum* (0.625); ESSP – *Eschweilera* spp. (0.828); RIGU – *Rinorea guianensis* (0.780); INLA – *Inga* cf. *laurina* (0.665); DIMA – *Dicypellium manausense* (0.559); LEGR – *Lecythis graciana* (0.826); ESTE – *Eschweilera* cf. *tasmani* (0.828); ANUN – *Andira unifoliolata* (0.760); BOMU – *Bocageopsis multiflora* (0.640); POCA – *Pouteria* cf. *caimito* (0.874); JACO – *Jacaranda copaia* (0.351); ESCO – *Eschweilera collina* (0.780); IRJU – *Iryanthera juruensis* (0.633); APTU – *Aptandra tubicina* (0.765); VIPA – *Virola pavonis* (0.587); CHKA – *Chaunachiton kappleri* (0.584); RUSP – *Ruizterania cassiquiarensis* (0.602); MISP – *Micropholis splendens* (0.884); EPGL – *Eperua glabriflora* (0.759); OUDI – *Ouratea discophora* (0.712); SIAM – *Simarouba amara* (0.712). Wood density (g cm⁻³) for each taxon given in parentheses; familial average used for *Dicypellium manausense*, and genus averages used for *Eschweilera* spp., *Eschweilera truncate*, *Ruizterania cassiquiarensis* and *Chaunachiton* sp.

average tree in a stand. Hale *et al.* (2012, 2015) presented a simplification of the GALES roughness method, which they termed the turning moment coefficient, or TMC method, which is suited to estimating individual-tree CWS and which we apply here because (a) it is an alternative approach to estimating CWS to the profile method used in HWIND, and (b) it can be used more easily with the available data than the original GALES model. The profile method used in HWIND calculates the wind loading on each height segment for trees based on a vertical wind profile; the total wind force is the sum of loading on each segment (for detailed comparison of the two methods, see Gardiner *et al.*, 2000). Because the profile method does not require inter-tree spacing information (the TMC method requires trees spacing information for calculating the *TMCratio*, see below), it may be a simpler approach in some circumstances for calculating loads on individual trees compared to the original GALES model; however, spacing indirectly influences the profile method calculation because LAI (see Equation (5) below) is a function of inter-tree spacing. Thus, all other things being equal, wind speeds inside the canopy of a widely spaced forest will be higher than in a denser stand.

An additional step presented here involves extending both approaches to estimate critical wind speeds for individual trees not only as snapshots (i.e. a static approach), but also in an iterative (i.e. dynamic) approach. Static methods calculate the CWS for each tree without consideration of the sequences of tree failure or change in the tree spacing or wind characteristics after one or more of the trees fall. Therefore, the original spacing and wind field is used for all trees. In contrast, an iterative or dynamic approach can allow for trees falling sequentially and incorporate the interactions between damage and altered wind beneath the residual tree canopy (Dupont *et al.*, 2015). Such a

dynamic approach would determine the first tree to fall, and then modify some components of the calculation to reflect changes in spacing or wind characteristics. Byrne and Mitchell (2013) and Seidl *et al.* (2014) illustrate applications of this approach in spatially explicit settings; our approach is used without spatially explicit tree locations and therefore cannot localize the effect of a tree's failure on its immediate neighbours. This is repeated after each tree failure, potentially resulting in dramatically different conditions for trees that fail much later in the process. This type of approach may be especially suited to stands made up of trees of numerous species and widely differing sizes and architectures, which are likely to fail sequentially across a range of wind speeds. Because our study trees fit this latter description, we added dynamic variants of both the profile and TMC methods.

Details of methods used

We define the critical wind speed as the wind speed necessary to generate a turning moment at the base of the trunk greater than or equal to the turning moment that resulted in tree failure in winching studies. The 'profile' method of estimating the critical wind speed is the basis of the HWIND model developed in Peltola *et al.* (1993) and Peltola *et al.* (1999). Each tree (both crown and trunk) is divided into a suite of vertical segments, usually 1 m in height. The standard formula for calculating drag on a vertical segment *z* m above ground from a purely horizontal wind is

$$D = 0.5 * \rho * C_d * A(z) * U(z)^2, \quad (1)$$

where *D* = drag (newtons), ρ = density of air (kg m⁻³), *C_d* = drag coefficient (dimensionless), *A*(*z*) = area (m²) of segment at height *z* and *U*(*z*) = wind velocity (m s⁻¹) at height *z*. An air

density of 1.1517 kg m^{-3} was used as representative of the warm, humid climate and low elevation (e.g. $\sim 90 \text{ m}$) in the vicinity of Manaus. Still-air drag coefficients decrease substantially as wind velocity increases and the crown streamlines, although they appear to reach a minimum asymptote (Cullen, 2005; Vollsinger et al., 2005); no applicable studies report drag coefficients at velocities above 20 m s^{-1} . Moreover, drag coefficients have not been measured for lowland tropical tree species. Instead, following Vollsinger et al. (2005), we estimated drag coefficients as declining from 0.75 at a wind velocity $>4 \text{ m s}^{-1}$, to 0.25 at a wind velocity of 20 m s^{-1} (drag coefficient is dimensionless). Note that this approach does not consider how drag might vary with leaf and canopy characteristics, nor defoliation of trees at elevated wind speeds.

Tree crowns were divided into 1 m segments starting from the top; the lowest segment usually was less than 1 m tall. For each segment, its area was used to calculate drag using the formula above. Crown segment areas were estimated as follows. Using crown area and crown depth, we calculated the width of an ellipse that would have the known area and a long axis equal to the crown depth; e.g. tree 14 was 25.5 m tall, had a crown depth of 9.3 m, and a crown area of 17.2 m^2 . An ellipse with 17.2 m^2 of area and 9.3 m length would have a short axis (width) of 2.36 m. Then using the semi-axes for ellipse length and width, the area of the first (top) crown segment was calculated as the area of an elliptical segment with a 'height' of 1 m. Areas of segments further from the top were the difference between, for example, areas of elliptical segments with 'heights' of $x \text{ m}$ and $x + 1 \text{ m}$. Similarly, trunks were divided into 1 m segments (again, the lowest segment was usually less than 1 m) starting from the top of the trunk. For trunk segments, we used the taper equations of Martin (1981, based on Kozak et al., 1969) to estimate trunk diameter at the top of the trunk (=height of crown base), and 1 m intervals downward from that point. These diameters were used to calculate segment areas as the product of the segment height (usually 1 m) and the average of the top and bottom diameter.

Predicted turning moments were calculated for canopy-top wind velocities between 5 and 130 m s^{-1} , in increments of 0.25 m s^{-1} .

The contribution of each vertical segment to turning moment at the tree base is the product of the drag produced directly by the wind and the height of the centre of that segment, plus an additional quantity – the mass overhang effect – caused by bending and the mass of the tree; these are summed across all vertical segments to yield total turning moment:

$$TM_{\text{total}} = \sum_{i=1}^S (D_{i,z} * z) + \sum_{i=1}^S (Mass_i * Defl_i * g) \quad (2)$$

where TM_{total} is the total turning moment (Nm), $D_{i,z}$ is the drag on segment i , whose centre is at height z ; $Mass_i$ is the mass of segment i (kg); $Defl_i$ is the lateral deflection of segment i (m) and g is the gravitational acceleration. We used Equations (5) and (6) from Peltola and Kellomaki (1993) to estimate lateral deflection of each 1 m vertical segment of each tree. The gravitational acceleration constant was 9.82 m s^{-2} . Masses of 1 m segments of each tree were measured in situ (Ribeiro et al., 2016). In most published CWS projections, the total basal turning moment (TM_{total}) resulting from each wind speed is

compared to tree resistances calculated separately for trunk and root system; in this study this step was slightly different because we sought to estimate the CWS for the actual trees that had been winched down in the Ribeiro et al. (2016) study. In other words, what wind speed would produce a TM_{total} that just exceeded the critical turning moment observed in the winching study? Therefore TM_{total} was compared directly to the M_{crit} values from Ribeiro et al. (2016), irrespective of the type of failure observed in the winching study, to determine critical wind speed (CWS).

In the turning moment coefficient (TMC) approach, it was necessary to calculate the critical wind speed separately for overturning and trunk breakage; this unavoidably differed somewhat from the direct comparison of TM_{total} to M_{crit} used for the profile method above. Therefore, we used Equations (11) and (12) from Hale et al. (2015) for calculating CWS for overturning and trunk breakage, respectively:

$$u_{\text{upr}}(h) = \left[\frac{C_{\text{reg}} * SW}{111.7 * dbh^2 * h} \right]^{1/2} \left[\frac{1}{1.136} \right]^{1/2} \left[\frac{1}{TMC_{\text{ratio}}} \right]^{1/2} \quad (3)$$

$$u_{\text{brk}}(h) = \left[\frac{\pi * MOR * d_0^3}{32 * 111.7 * dbh^2 * h} \right]^{1/2} \left[\frac{f_{\text{knot}}}{1.136} \right]^{1/2} \left[\frac{1}{TMC_{\text{ratio}}} \right]^{1/2} \quad (4)$$

where u_{upr} = critical wind velocity (m s^{-1}) for uprooting; u_{brk} = critical wind velocity (m s^{-1}) for trunk breakage; h = total tree height (m); C_{reg} = regression coefficient obtained when regressing (forced through origin) critical turning moment (Nm) against stem mass (kg); SW = stem weight (kg); dbh = trunk diameter at 1.4 m (m); d_0 = trunk diameter at ground level (m); MOR = modulus of rupture (Pa); and f_{knot} = knot factor to reduce trunk strength due to knots (dimensionless; here set to 0.9). TMC_{ratio} (as in Hale et al. (2015) represents the change in wind loading after thinning (in their usage), or after a subset of the trees have fallen (in our usage for the dynamic analyses); because the study site was unmanaged and undisturbed forest, the third term in Equations (3) and (4) above is unity in the static analyses. Once u_{upr} and u_{brk} were calculated from Equations (3) and (4) above, the one was chosen that matched the type of damage observed for that tree in the winching study and that quantity was considered the static TMC estimate of CWS for that tree. Of the winched trees in Ribeiro et al. (2016), one third uprooted and two thirds exhibited trunk breakage.

Modulus of rupture (MOR) values have been directly measured and reported for only a subset of tropical moist forest species. When available (e.g. from Chudnoff, 1984), we used the reported MOR value for a given taxon. When such values were not available, we estimated MOR from wood specific gravity for a given taxon. Using data in Chudnoff (1984) for 110 South American tropical wet forest species for which modulus of rupture and wood specific gravity are both known, we regressed MOR on specific gravity and obtained a predictive equation with $R^2 = 0.805$; we then applied that predictor to the wood specific gravity of our study species, drawn from the Global Wood Density Database (URL: <http://discovery.ucl.ac.uk/id/eprint/1453390>; DOI: 10.5061/dryad.234).

We report critical wind speeds at mean canopy height (i.e. 30 m) for consistency with existing studies.

The profile method requires a wind profile, to calculate the wind velocity and therefore drag on each 1 m vertical segment of a given tree. We utilized the most recent and most geographically relevant estimate of wind profile, reported in [de Santana et al. \(2017\)](#). Their Equation (6) gives the Modified Souza Model and is

$$u(z) = \bar{u}_h \left\{ \left[\frac{-1 + \exp(\mu z)}{\exp(z)} \right] * \tanh \left[\beta + \exp \left(-LAI \left(1 - \frac{z}{z_{ip}} \right) \right) \right] \right\} \quad (5)$$

where μ and β are constants given by the authors as 1.012 and 0.1, respectively, z is the height above ground (m) and z_{ip} is the height of the inflection point (m), which is equal to the mean canopy height (30 m). Based on LAI values reported in [Filho et al. \(2005\)](#) and [Tóta et al. \(2012\)](#) for Amazon forests, an undisturbed LAI of 6.7 was used.

As a benchmark against which to compare CWS estimates from the four analyses described above, we also calculated CWS for the set of 60 trees by the static profile method, but assuming open (non-forest) surroundings. The procedure was the same as for the static profile method described above, but rather than the wind profile from [de Santana et al. \(2017\)](#), we used a basic logarithmic profile as described in [Peltola \(2006\)](#):

$$u(z) = \left(\frac{U_0}{k} \right) * \left(\ln \left(\frac{z}{z_0} \right) \right) \quad (6)$$

where k = von Karman's constant (0.4, dimensionless); U_0 = friction velocity (calculated by solving for U_0 when 'ambient' wind speed is specified at a height of 40 m; $m s^{-1}$); z_0 = roughness length (0.05, units of m). The roughness length value was based on the assumption of predominantly low vegetation such as tall grass.

Parameter values used in our calculations are given in Table 1. We carried out an informal test of the sensitivity of our CWS results to the drag coefficient and leaf area index (LAI), as well as three tree morphological descriptors (height, crown depth, and crown width), by decreasing or increasing the focal parameter by 20 per cent, and recording the change in CWS compared to that resulting from the default parameter value. Subsequently, to further explore the effect of drag coefficient on CWS estimates, we substituted the range of drag coefficients reported by [Kane et al. \(2008\)](#), i.e. 0.63–0.43 (lower to higher wind speeds), instead of the range (from [Vollsinger et al., 2005](#)) originally used.

Iterative (dynamic) analyses

To apply the profile method dynamically, a custom C++ programme was written, which looped through canopy-top wind speeds from 5 to 130 $m s^{-1}$ in increments of 0.25 $m s^{-1}$. At each canopy top wind speed, wind load was calculated on each tree and predicted basal turning moment compared to the empirically measured critical turning moment. If the predicted turning moment was greater, the tree was declared fallen. Following each tree failure, several parameters were adjusted to account

for the altered spacing and wind characteristics. Tree spacing was adjusted, which in turn altered the gust factor. Because the taller trees fell at lower wind speeds, mean canopy height was recalculated after each tree failure, and this was reflected in an identical change in the inflection height (z_{ip}) in Equation (5). Finally, since each tree failure reduced canopy density in the stand, leaf area index was adjusted: the total crown areas of all remaining sample trees was summed and the initial LAI (6.7) was multiplied by the proportion of initial crown area that remained standing. For example, the sum of initial crown areas for the 60 study trees was 2075.5 m^2 ; if after several failures the sum of crown areas was 1900 m^2 , the adjusted LAI would be 6.7 * (1900/2075.5) = 6.133. Thus the wind profile would be altered by the modified values for z_{ip} and LAI, while modified spacing would alter the gust factor.

To apply the TMC iteratively, Equations (3) and (4) above were used to calculate preliminary CWS for uprooting vs. trunk breakage, and for each tree, the CWS was chosen that corresponded to the type of tree failure observed for that tree in the winching study. For example, tree 12 failed by trunk breaking, therefore the CWS for trunk breakage from Equation (4) was chosen for use in the dynamic TMC analysis. In Equations (3) and (4) above, $TMCratio = 0.99 * spacing_ratio$. $spacing_ratio$ is in turn the ratio of tree spacing after, to tree spacing before, removal of one or more trees. Thus as an example after four trees had failed: spacing is 4.138 m for a starting density of 584 trees ha^{-1} (see Study site and Methods section above) and 4.152 m for a density of 580 trees ha^{-1} , $spacing_ratio$ would be unity before the first tree failure, and later would be 0.9966 after four trees had failed. One tree failure comprised a single iteration; in each iteration, the tree with the lowest CWS (matched to observed type of failure in the winching study) was selected, declared failed and removed from further consideration. After each successive tree failure, an adjusted spacing was calculated for trees that remained standing, and used to calculate a new spacing ratio. Thus, the first two terms in Equations (3) and (4) remained constant across iterations, while the third term changed after each tree failure. Iterations continued until all trees failed.

These estimates of CWS implicitly assumed the winched trees were growing together in an imaginary stand, but such a stand lacked any location information for individual trees. An unavoidable consequence of this is that changes to the wind profile were uniform throughout the imaginary stand, whereas in real forest stands, the effects of loss of a tree (particularly the first few trees) would be much more localized.

We used Mann–Whitney rank sum tests to test for differences in estimated CWS between the two taxa of interest, because assumptions of parametric t -tests were violated.

Results

Among all species pooled, height varied between 18.1 m and 31.3 m, with a mean of 25.2 ± 3.1 m (Table 2). The height of *Eschweilera* spp. trees covered almost the full spectrum of the entire data set, with a minimum of 18.09 m, a maximum of 30.7 m and mean of 24.1 ± 3.2 m. *S. micranthum* had a minimum and maximum height of 20.6 m and 31.3 m, respectively. The mean was 25.7 ± 3.2 m. Tree height for all individuals

pooled was strongly correlated with dbh ($r = 0.591$, $P < 0.001$), but only weakly correlated with crown area ($r = 0.286$, $P = 0.028$). For the genera of special interest, the dbh-height correlations were far stronger: $r = 0.748$ and $P < 0.001$ for *Eschweilera* spp., and $r = 0.849$ and $P < 0.001$ for *S. micranthum*. Height:diameter ratios ranged from roughly 55 to greater than 120; notably, in contrast to expectations (e.g. Kenk and Guehne, 2001; Mason, 2002) that taller and, particularly, dominant trees have lower height:diameter ratios, height:diameter ratios did not decrease with tree height (no significant correlation).

The study trees varied more than 13-fold in vertical crown cross-sectional area (range 6.3 m², a *Jacaranda copaia*, to 86.7 m², a *Dicypelium manauensis*), despite having a range of only 22 cm (19.0–41.1 cm) in diameter at breast height (Table 2); as a result, for all species pooled there was no correlation between dbh and crown area ($r = 0.228$, $P = 0.082$). Among the genera of interest, *Eschweilera* spp. exhibited no correlation between dbh and crown area ($r = 0.337$, $P = 0.146$), but there was a strong relationship for *S. micranthum* ($r = 0.625$, $P = 0.004$). The mean crown cross-sectional area for all species pooled was 34.8 ± 19.3 m² (mean \pm sd) and for *Eschweilera* spp. and *S. micranthum* was 45.1 ± 22.4 and 25.1 ± 9.6 m², respectively. The range in crown area for *Eschweilera* spp. was 15.3–85.1 m², while that of *S. micranthum* was 11.6–41.3 m². While both crown depth and crown width were quite variable and thus contributed to the high variability in crown area, width was more variable (coefficient of variation = 0.401) than depth (coefficient of variation = 0.231).

Critical turning moments reported in Ribeiro et al. (2016) ranged from 32 375 N to 372 447 N, with a mean of 171,192 (± 87 325 N) for all species pooled (Table 2). For *Eschweilera* spp. and *S. micranthum*, mean critical turning moments were 182,651 (± 88 520) N and 186 342 (± 92 354) N, respectively. These indicators of tree ‘strength’ were very strongly correlated with tree dbh for all species pooled ($r = 0.819$, $P = 0.0004$). Similarly, for *Eschweilera* spp. only, the dbh-turning moment correlation was strong ($r = 0.845$, $P = 0.0008$), as it also was for *S. micranthum* ($r = 0.939$, $P = 0.0002$).

Static analyses

CWS estimated with the static ‘profile’ method varied more than tenfold among the study trees (all species pooled), with a minimum of 10.75 m s⁻¹, and maximum of >120.0 m s⁻¹ (Figure 1). The mean was 45.70 ± 26.90 m s⁻¹. For *Eschweilera* spp., the minimum, maximum, and mean were 14.0 m s⁻¹, 117.25 m s⁻¹ and 46.77 ± 22.12 m s⁻¹, respectively, while for *S. micranthum*, the same values were 26.00 m s⁻¹, 118.0 m s⁻¹ and 52.94 ± 29.03 m s⁻¹, respectively. CWS estimated with the static profile method were negatively correlated with height:diameter ratios of the study trees ($r = -0.347$, $P = 0.007$, $n = 60$).

CWS were much lower when the wind profile of open surroundings was used. The mean and standard deviation of CWS in this scenario were 14.20 ± 6.41 m s⁻¹; the two lowest CWS were both 7.0 m s⁻¹, and the two highest were 31.25 and 31.5 m s⁻¹.

CWS (at mean canopy height of 30 m; not 10 m above zero plane displacement as in Hale et al., 2015) estimated with the static TMC method were much less variable among trees

(Figure 1); the minimum and maximum were 18.98 and 52.01 m s⁻¹, respectively, and the mean was 30.88 ± 7.51 m s⁻¹ for the full data set (Table 2). Minimum, maximum, and mean were 19.44, 52.01 and 31.77 ± 9.00 m s⁻¹ for *Eschweilera* spp., and 25.40, 39.90 and 32.10 ± 4.09 m s⁻¹ for *S. micranthum*.

Thus for the study trees, mean critical wind speeds from the static TMC method were very similar for the two genera of interest (31.77 vs. 32.10 m s⁻¹), while means calculated with the static profile method diverged more widely (46.77 vs. 52.94 m s⁻¹). Nevertheless, testing for differences between the two focal taxa (*S. micranthum* vs. *Eschweilera* spp.) found no significant differences for CWS estimated with either the static profile or the static TMC methods (Mann–Whitney rank sum tests; $P > 0.05$ in both cases).

Dominance (based on rank when study trees were ranked from shortest to tallest, i.e. tallest = 60) was negatively correlated to the CWS estimated from the static profile method ($r = -0.578$, $P < 0.001$, $n = 60$), although for the CWS estimated from static TMC method, there was no significant correlation ($r = -0.016$, $P = 0.90$).

Dynamic analyses

Results of the dynamic analyses differed substantially from the static analyses, primarily in a far smaller range of CWS among the study trees, along with lower means (Figure 1 and Table 2). For all species pooled, the mean, minimum and maximum CWS from the dynamic profile method were 22.60 ± 4.34 m s⁻¹, 10.75 m s⁻¹ and 34.50 m s⁻¹, respectively. The corresponding values for *Eschweilera* spp. were 22.54 ± 3.82 m s⁻¹, 13.50 m s⁻¹ and 34.50 m s⁻¹; and for *S. micranthum* were 24.49 ± 3.69 m s⁻¹, 20.00 m s⁻¹ and 33.25 m s⁻¹. *S. micranthum* and *Eschweilera* spp. were significantly different from one another for CWS estimated with the dynamic profile method (Mann–Whitney rank sum test, $P = 0.026$).

CWS estimated from the dynamic TMC method were the least variable of the four methods (Figure 1 and Table 2). Mean, minimum and maximum values for the full data set were 25.01 ± 2.21 m s⁻¹, 18.98 m s⁻¹ and 29.59 m s⁻¹, respectively. *Eschweilera* spp. CWS ranged from 19.46 to 28.69 m s⁻¹, with a mean of 24.96 ± 2.43 m s⁻¹, while the range for *S. micranthum* was 23.78–27.65 m s⁻¹, with a mean of 25.95 ± 1.20 m s⁻¹. The CWS estimated with dynamic TMC method did not differ between *S. micranthum* and *Eschweilera* spp. (Mann–Whitney rank sum test, $P = 0.250$).

As with the static analyses, for the dynamic analyses, dominance was significantly negatively correlated ($r = -0.388$, $P = 0.002$) with the dynamic profile CWS, but not significantly related to dynamic TMC CWS ($r = -0.051$, $P = 0.70$).

Sensitivities

Using the original static profile CWS estimates as the default, varying five of the input parameters produced mean changes up to 85 per cent in CWS (Table 3). Decreases and increases in drag coefficient caused CWS to increase by an average of roughly 17 per cent or decrease by an average of roughly 12 per cent, respectively. When LAI was increased or decreased 20 per cent, resulting CWS estimates changed an average of 17.5 per cent. Among the morphological input variables, tree height had by far the greatest impact on CWS estimates: varying height by 20 per cent produced

an increase of 85 per cent and decrease of 58 per cent for lower and higher heights than the default, respectively. Crown depth was the least influential of the morphological variables. Increases and decreases of crown depth by 20 per cent caused mean increases of 3.6 per cent and mean decreases of 1.1 per cent in CWS. Finally, 20 per cent increases or decreases in crown width yielded 17.4 per cent increases, and 12.4 per cent decreases, respectively, in CWS.

Discussion

Most reports of critical wind speeds estimated from models are based on the GALES or HWIND (Peltola and Kellomaki 1993; Peltola et al. 1999) or FOREOLE (Ancelin et al., 2004) models (Table 4). GALES has been the most widely applied wind risk

model and has been the tool for critical wind calculations in the UK (Gardiner et al., 2000, 2008), France (Ancelin et al., 2004), Quebec (Ruel et al., 2000), British Columbia (Byrne and Mitchell, 2013), Japan (Kamimura et al., 2008) and Spain (Locatelli et al., 2016). Byrne and Mitchell (2013) have generalized GALES for use in multi-species temperate plantations but no previous study has been done in hyperdiverse tropical forests with complex structure. Indeed, with the exception of Locatelli et al. (2016), who parameterized the model for *Eucalyptus globulus* plantations, all existing critical wind speed estimates using GALES have been with conifer species. Locatelli et al. (2016) and Peltola et al. (1999, studying birch stability in Finland) appear to be the only previous attempts to use the HWIND model to estimate critical wind speeds for broadleaf trees. This limited attention to broadleaf trees may be especially important in hyperdiverse tropical forests, where numerous species traits undoubtedly vary much more widely than in low-diversity cool-temperate forests and plantations. For example, of the 23 architectural types enumerated for trees by Hallé et al., 1978), all are found in the tropics but many are absent from temperate-zone forests (Tomlinson, 1983).

Although most early applications of GALES and HWIND were at the stand level, recent efforts have begun to place more emphasis on applying these models to individual trees (Ancelin et al., 2004; Byrne and Mitchell, 2013; Hale et al., 2012, 2015; Kamimura et al., 2016, 2017). There are currently six modeling options to calculate critical wind speeds for individual trees in a stand, based on variability in size, and some cases, location and neighbourhood: the profile approach from HWIND (Peltola et al., 1999), the FOREOLE model (Ancelin et al., 2004), ForestGALES/BC (Byrne and Mitchell, 2013), the TMC modification of GALES by Hale et al. (2015), ForGEM (Schelhaas et al., 2007) and iLand (Seidl et al., 2014). ForestGALES/BC and FOREOLE have not yet been parameterized for use outside of the regions and vegetation types for which they were developed (British Columbia and France, respectively). ForGEM and iLand require spatially explicit tree locations to operate; such information was not available in our study. The TMC modification of GALES, however, could be used in the case of our Amazonian forest site, given the types of data available to us. Thus, we used the TMC approach to estimate CWS, in addition to the ‘profile’ method, to develop two

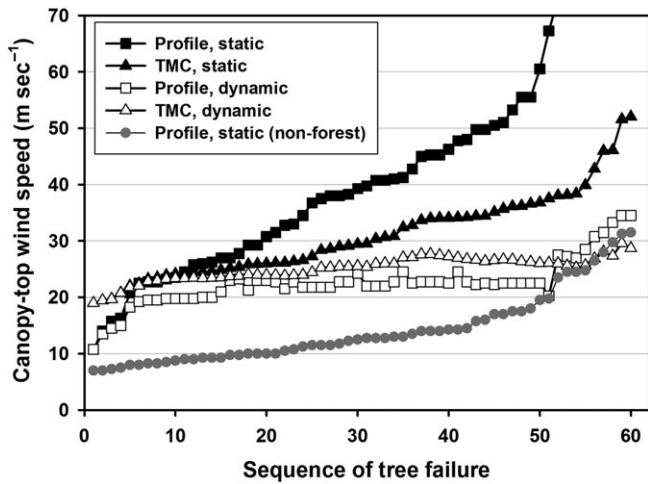


Figure 1 Canopy top critical wind speeds estimated for 60 Amazon moist forest trees, using five different estimation methods. Trees ordered from first to last tree to fail with increasing wind speeds. For dynamic CWS estimates, the failure of a tree occasionally results in the next tree failing at lower wind speeds because of changes in spacing and the wind characteristics.

Table 3 Sensitivity of CWS estimates to variation in drag coefficient and tree morphology parameters.

Parameter	25th percentile	Median	75th percentile	Mean change in CWS ¹
Default, all	27.00	39.50	50.75	Does not apply
Drag coefficient -20%	31.12	47.00	60.12	17.45 ± 3.01%
Drag coefficient +20%	24.25	34.38	44.37	-12.38 ± 2.23%
Height -20%	55.62	70.38	86.0	84.69 ± 41.52%
Height +20%	10.62	15.38	22.25	-58.24 ± 6.20%
Crown depth -20%	27.75	41.13	53.62	3.61 ± 4.44%
Crown depth +20%	26.87	39.13	51.12	-1.15 ± 2.70%
Crown width -20%	31.12	47.00	60.12	17.45 ± 3.01%
Crown width +20%	24.25	34.38	44.37	-12.38 ± 2.23%
Leaf area index -20%	22.88	32.50	40.75	-17.52 ± 3.51%
Leaf area index +20%	31.50	46.88	59.62	17.52 ± 3.51%

¹Mean (n = 60) change in estimated CWS relative to default.

Table 4 Estimates of critical wind speed from published literature.

Study	Species	Type of damage	Constant ^b	Variable ^b	Model	Critical wind speed, m s ⁻¹
Peltola et al. (1999) ¹	<i>Pinus sylvestris</i>	Uproot	Height = 16 m	Ht/dbh = 80–120	HWIND	20.0–31.0
		Break	Ht/dbh = 100 Height = 16 m Ht/dbh = 100	Height = 12–20 m Ht/dbh = 80–120 Height = 12–20 m		23.0–29.0 21.0–35.0 25.5–27.5
Ancelin et al. (2004)	<i>Picea abies</i>	Uproot	Height = 20 m	Ht/dbh = 120–80	FOREOLE	10–18
		Break	Ht/dbh = 100 Height = 20 m Ht/dbh = 100	Height = 12–20 m Ht/dbh = 120–80 Height = 12–20 m		12–14 8–20 11–14
Locatelli et al. (2016)	<i>Eucalyptus globulus</i>	Both		Height = 5–25 m; density = 300–3300 stems ha ⁻¹	ForestGALES	12–112
Achim et al. (2005)	<i>Abies balsamea</i>	Uproot		Age = 40–145 year; Height = 14.0–21.0 m; dbh = 14.1–23.3 cm	GALES	18–20
Gardiner et al. (2000)	<i>Picea abies</i>	Uproot	Height = 20.0 m	Ht/dbh = 80–120	GALES	14.0–22.0
		Break	Height = 20.0 m	Ht/dbh = 80–120		22.5–23.5
		Uproot	Ht/dbh = 100	Height = 12–20 m		16.5–17.0
Cucchi et al. (2005)	<i>Pinus pinaster</i>	Break	Ht/dbh = 100	Height = 12–20 m	GALES	16.0–16.5
		Uproot	Ht/dbh = 100	Age = 20–50 year; height = 13.5–27.1 m; dbh = 19.5–48.4 cm; Ht/dbh = 70.0–54.1		19.5–31.5
Schelhaas et al. (2007)	<i>Pseudotsuga menziesii</i> ^c	Both	Age=60 year; density = 656 stems ha ⁻¹	Dbh = 26.2 ± 11.6 cm; height = 24.4 ± 8.77 m	ForGEM (from HWIND)	10–40
Dupont et al. (2015)	<i>Pinus sylvestris</i>		Ht/dbh = 100; Height = 20 m	Shelter stand vs. clearcut upwind	HWIND	20–32
			Ht/dbh = 100; Height = 20 m	Shelter stand vs. clearcut upwind		16–50
Hale et al. (2015)	<i>Picea abies</i> <i>Picea sitchensis</i>	Uproot			ForestGALES - TMC	26.4–43.3 (25th–75th %iles)
Seidl et al. (2014)	<i>Picea abies</i>	Both	Dbh = 30 cm	Height = 15–40 m	iLand	12–22

¹Stand interior or no gap.²Heights in m, dbh in cm, density in N ha⁻¹.^cUnmanaged stands.

independent static estimates of CWS for our study trees. Each of these two approaches was then extended to estimate CWS dynamically, accounting for previous tree falls.

Overall, our estimates of critical wind speeds fall in the range or are slightly higher than CWS of other reports for mature trees growing in temperate plantations (Table 4); this difference became much larger for the last 10–15 trees to fail in our data set. For example, [Achim et al. \(2005\)](#) reported critical wind speeds $15\text{--}18\text{ m s}^{-1}$ for 40-year-old stands of balsam fir in Canada; these values decreased further in the oldest stands, to as low as 10 m s^{-1} for 140 year-old stands. [Ancelin et al. \(2004\)](#) found that critical wind speeds varied as a function of tree slenderness and height, from <10 to $\sim 24\text{ m s}^{-1}$ for trees between 12 m and 20 m tall and with slenderness (height/diameter) between 80 and 120. [Hale et al. \(2015\)](#) found that their TMC approach produced critical wind speeds between 26 and 43 m s^{-1} (first to third quartiles) for mixed conifer stands in Scotland (minimum and maximum of 10.5 and 100.0 m s^{-1} , respectively). [Kamimura et al. \(2017\)](#) used the TMC approach to estimate individual-tree CWS of approximately $19\text{--}26\text{ m s}^{-1}$ for *Larix kaempferi* trees in Japan. One of the few studies focused on broadleaf trees ([Locatelli et al., 2016](#)) found that for *Eucalyptus globulus*, critical wind speeds for 25 m tall trees ranged from $\sim 37\text{ m s}^{-1}$ (when tree density was 300 stems ha^{-1}) to 22 m s^{-1} ($1650\text{ stems ha}^{-1}$). Given the differences between our study and [Locatelli et al.](#), it is encouraging that our findings of most CWS in the range of $20\text{--}27\text{ m s}^{-1}$ is broadly similar to theirs.

The CWS obtained using a non-forested wind profile in a static profile analysis are much lower, dramatically illustrating the effect of growing in a closed stand. It is noteworthy that comparing the original static profile results to the non-forested static profile results in this study reveals sheltering effects, i.e. effects of neighbouring trees on the wind profile, but does not take into consideration crown collisions or mutual support. Such a comparison must be evaluated carefully, however, because the tree dimensions observed for the study trees would almost certainly not be the dimensions the same trees would exhibit had they grown in non-forest conditions throughout their lives.

Among the tree characteristics that influence critical wind speed, tree height, slenderness and trunk diameter have been emphasized the most, but crown area has also received a modest amount of attention. While several studies (including results presented here) agree that tree height is perhaps the foremost morphological trait determining tree CWS (e.g. [Locatelli et al., 2016](#); [Kamimura et al., 2017](#)), this study reinforces the value of considering crown area as well. Notably, earlier work by [Dunham and Cameron \(2000\)](#) points in the opposite direction from our findings, i.e. that trees with smaller crowns were more vulnerable than trees with large crowns. [Kamimura et al. \(2017\)](#) examined effects of crown length and width independently on tree damage using logistic regression and found that tall trees with shorter crown lengths (vertical dimension) were more likely to be damaged, apparently because of the resulting shift of the centre of pressure higher on the tree. Conversely, [Bonnesoeur et al. \(2013\)](#) found that damage probability increased slightly with increasing crown width for *Fagus sylvatica* in France.

Sensitivity analyses have provided a basis for comparing the influence of various input parameters on the CWS estimates produced. [Peltola et al. \(1999\)](#), found that altering crown width

or crown depth in HWIND by 20 per cent produced changes in predicted critical wind speeds of 6.8–23 per cent, and 3.2–15.7 per cent for uprooting and trunk breakage, respectively. [Gardiner et al. \(2000\)](#) found that varying crown depth by 20 per cent in GALES and HWIND resulted in 0–12 per cent variation in estimated CWS, while varying crown width resulted in 0–23 per cent variation in estimated CWS. Our informal sensitivity analyses (Table 3) found that varying tree height had dramatic effects on CWS estimates, but also that variation in crown width produced important changes in CWS (i.e. 20 per cent increase in crown width produced 12 per cent decrease in CWS, on average); the decrease in CWS with increasing crown width is not due to smaller trunk diameters for wide-crowned trees (no correlation between crown width and dbh: $r = 0.110$, $P = 0.404$). [Locatelli et al. \(2017\)](#) presented a thorough sensitivity analysis of the ForestGALES model to input parameters, suggesting substantial effects of crown area. Given that our results as well as those in [Peltola et al. \(1999\)](#) and [Gardiner et al. \(2000\)](#) suggest something between 0.5:1 and 1:1 correspondence between variation in crown width and estimated CWS, the nearly 14-fold range in crown areas of our study trees may be expected to produce a wide range in our estimates of CWS. Conversely, in managed forests where crown width variation is often modest and trees are typically regularly spaced and of similar age, crown area probably varies much less than in this study, and consequently may cause little variation in CWS in such conditions.

Our results imply that in diverse tropical forests, crown area may be an important influence on trees' wind vulnerability. For example, if our study trees are ordered from smallest to largest in terms of crown area, the largest five have an average crown area that is 6.8-fold greater than the average crown area of the smallest five. At an arbitrarily-chosen wind speed (25 m s^{-1}), the five largest and five smallest have a 7.5-fold difference in predicted basal turning moment. Acclimative growth would suggest that such variation would be compensated by stronger trunks or root systems. Yet, the calculated critical trunk strength showed only a roughly 3-fold difference between the two groups, and the observed critical turning moments (measured via winching) showed only a 2.5-fold difference. Moreover, height:diameter ratios, which would be expected to be lower for the tallest trees if they are fully acclimated (e.g. [Kenk and Guehne, 2001](#); [Mason, 2002](#)), are not negatively correlated with tree height in our sample. These trends suggest that for at least the extreme large-crowned trees, trunk and root system strength may be insufficient to compensate for the larger crown, resulting in a subset of large, vulnerable trees ('large' in this context means perhaps 40 cm dbh or greater). This does not necessarily contradict the well-established observation that wind loading during growth causes trees to increase radial growth and therefore stability, resulting in acclimation to the wind environment. Instead, when high wind events are occasional with long time periods between events at a given location, tree growth will be acclimated to a low-wind situation, and may result in some trees being vulnerable when the high wind events do occur.

This variation in crown areas has implications for forest disturbance dynamics. On the one hand, close-spaced trees of uniform size are likely to form a closed canopy that deflects most of the wind over the top of the canopy ([Quine and Gardiner, 2007](#)). On the other hand, when variation in stand structure,

crown area and other key species-traits (e.g. wood density, maximum tree height/size and leaf traits) is higher, the more vulnerable individuals will likely be the first to fall in a wind event, thereby opening the canopy for entry of wind and propagation of the initial gaps (Silverio *et al.*, 2019). Such a process would result in a steady increase in the proportion of a stand downed as wind speed increases, whereas plantations with lower species diversity and less structural variability are more likely to exhibit thresholds of CWS in which there is a rapid transition from little damage to extensive damage across a small increment in wind speed. Taken a step further, a potential ecological implication is that management or natural disturbances that result in low diversity and simplified structure will produce stands with threshold wind speed-damage relationships. Whether such diversity promotes forests to be more resilient overall will depend on numerous factors such as size distributions, inter-tree spacing and interspecific variation in architecture and wood properties.

Seeking to address shortcomings of an entirely static approach to estimating CWS, this study presented two ways (one was a dynamic variant of the profile method, and the other a dynamic variant of the TMC method of Hale *et al.*, 2015) to implement a dynamic estimation of CWS, which considers propagation of tree damage through a stand, and thus changes in spacing and wind characteristics. Alternative and spatially explicit implementations of a dynamic approach have been given in Byrne and Mitchell (2013), Seidl *et al.* (2014) and Kamimura *et al.* (2017). The results of our dynamic profile estimations of CWS were, as expected, much more truncated than the results of the static profile CWS (Figure 2). This should be true, because as initial trees fail, wind can enter the stand and increase loading of the remaining trees. Thus, we suggest that the static approaches probably will be unsatisfactory for estimating CWS of trees that fail late in the process of extensive or complete canopy destruction. Whether the implementation used here to model propagation is satisfactory or not is still unknown, and some limitations are discussed below.

The primary motivation for this work was to determine if a mechanistic basis could be found for recent thinking that wind disturbance is widespread in Amazonian forests (Chambers *et al.*, 2013; Magnabosco Marra *et al.*, 2014; Rifai *et al.*, 2016). Building on data from the Ribeiro *et al.* (2016) static winching study, we estimated that the study trees would begin to fall at wind speeds exceeding 11 m s^{-1} . If critical wind speeds in the range that we estimated here are common, then it is indeed likely that wind may be a major driver of Amazonian forest dynamics. Garstang *et al.* (1998) found that convective downbursts in the Amazon commonly produce winds in the range of $20\text{--}25 \text{ m s}^{-1}$, and occasionally up to 31 m s^{-1} . Similarly, Negrón-Juárez *et al.* (2010) estimated that a January 2005 squall line that crossed much of the Amazon basin produced winds up to 41 m s^{-1} . Using results from the static profile method, 30 m s^{-1} winds would be sufficient to topple almost one third of the trees in our data set. Alternatively, results from the dynamic profile method would predict that 30 m s^{-1} winds down > 90 per cent of our trees. However, two caveats should be noted: one, that wind speeds measured from meteorological stations in open conditions may be higher than actual wind speeds experienced by trees (Albini and Baughman, 1979), and two, that the HWIND and GALEs models calculate the critical mean hourly

wind speeds rather than instantaneous wind speeds. Therefore, the results reported here cannot be directly compared to meteorological observations. Nevertheless, the intermingling of trees with widely divergent critical wind speeds, and overlap between meteorological observations and calculated CWS implies that, other factors being equal, intermediate-intensity storms should topple an intermediate fraction of trees in an affected area, and lead to the observation that small gaps are far more common than large blowdowns across the Amazon (Silverio *et al.*, 2019).

Limitations

Several factors likely limited the precision of our estimates of critical wind speeds and reveal a need for further research.

First, for the estimates presented here, we used published drag coefficients (Vollsinger *et al.*, 2005) that were based on small saplings (3–5 m tall) of temperate species different than those used in this study. Kane *et al.* (2008) measured drag and calculated drag coefficients for three hardwood species in a less-controlled experiment; they reported a mean drag coefficient of 0.627 at very low-wind speeds, decreasing to a mean of 0.43 at 20.0 m s^{-1} . When our static profile estimates of CWS were recalculated using the Kane *et al.* range of drag coefficients, the CWS decreased an average of 13.6 per cent compared to when the Vollsinger *et al.* drag coefficients were used. Consequently, while the original Vollsinger *et al.* drag coefficients (0.25–0.75) produced mean CWS of $45.7 \pm 26.6 \text{ m s}^{-1}$ for all trees, this decreased to $38.0 \pm 18.8 \text{ m s}^{-1}$ for the Kane *et al.* drag coefficients. Clearly equally plausible estimates of a range of drag coefficients can result in substantially different estimates of CWS.

Second, like all existing models, both our profile and TMC calculations are based on critical turning moments from static winching, which does not address the potentially important influence of tree swaying and resulting loosening of the root-soil interface. If swaying does indeed cause substantial loosening of the root system and, therefore, loss of wind resistance, then the duration of a storm becomes especially important, and during long-lasting storms our estimates of critical wind speeds may be overestimated.

Third, although our static profile and TMC approaches do not consider the effect of neighbours on critical wind speed estimates, the dynamic variants of these approaches are a step toward estimates that consider surroundings, even in the absence of spatially explicit tree locations (for alternative ways to address propagation, see Byrne and Mitchell, 2013; Seidl *et al.*, 2014, and Dupont *et al.*, 2015). Neighbours may have several, potentially contradictory, effects on an individual tree's CWS. On the one hand, neighbours could benefit a focal tree by providing mechanical support or shelter from winds; both of these effects would increase the focal tree's CWS. Alternatively, over a longer time frame, neighbours could make a focal tree more slender (if neighbourhood density is high), thereby decreasing the focal tree's CWS. The dynamic CWS estimates presented here begin to address the sheltering effect by modifying the wind profile and gust factor as well as mean canopy height as increasing numbers of trees are toppled by the wind, whereas mechanical support and neighbour effects on

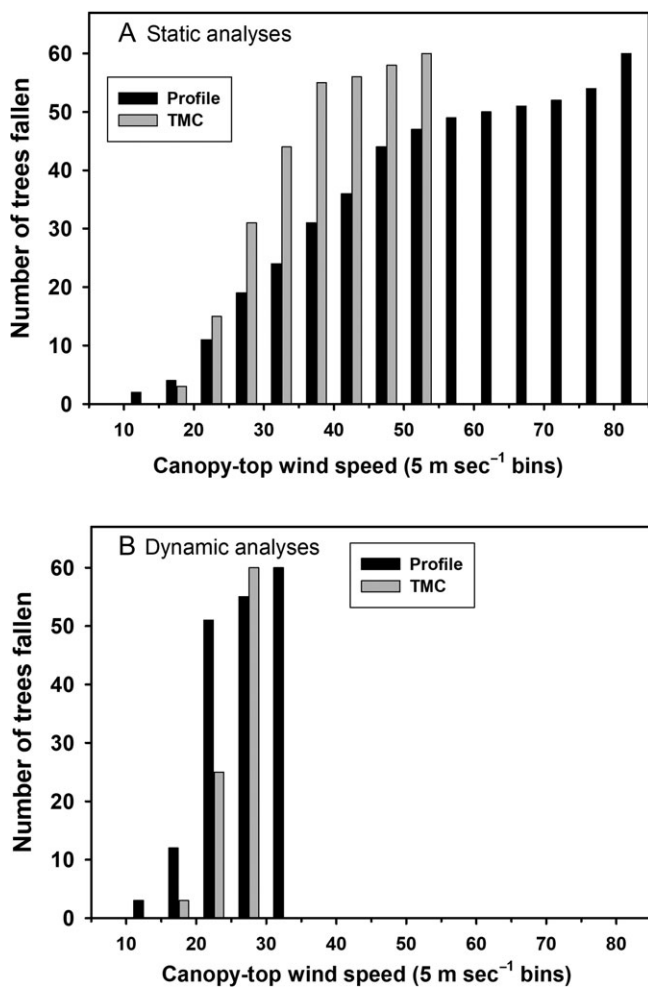


Figure 2 Cumulative number of trees fallen (out of 60) at increasing wind speeds, in bins of 5 m sec^{-1} . Top panel: static profile and TMC analyses; bottom panel: dynamic profile and TMC analyses.

morphology are not yet addressed (but see [Schelhaas et al., 2007](#)). In our opinion, both the static and dynamic approaches presented here have shortcomings: the static approach produces unrealistically high CWS estimates for the last one third of the trees to fall, whereas, the dynamic approach may open the stand too quickly, causing the distribution of CWS among trees to be unrealistically narrow (i.e. once trees begin to fall, the entire stand is down after very small further increases in wind velocity). These two approaches might be best thought of as extremes in terms of modeling iterative treefall processes; possibly the best approach lies in between the two extremes given here. Very recent results from [Hart et al. \(2019\)](#) using random forests and artificial neural networks look especially promising in this regard; notably, these researchers conclude that at their study sites in France, damage occurs at the stand scale, with limited importance of individual-tree characteristics.

Fourth, tree stability likely has a complex and contingent relationship to soil moisture and saturation. While some findings indirectly infer that saturated soils may substantially weaken root system wind resistance (e.g. [Foster, 1988](#)), saturated soils are heavier than dry soils and therefore the additional weight

may add stability to a tree. Currently it is unknown whether saturation will lead to decreased stability, but since high winds in Amazonian forests are overwhelmingly associated with storms that produce precipitation, it is likely that trees in our study site experience wind effects in the context of very wet soils.

Last, our estimates of dynamic CWS assumed that the winched trees were growing together in an imaginary or ‘virtual’ stand. Doing so allowed consideration of changes in the wind profile as trees progressively failed, but because of the lack of locations for individual trees, the wind profile changes were the same for all of the remaining trees in the virtual stand. In a real stand of trees, the wind profile changes would be experienced by near neighbours but not trees further away; this limitation seems an unavoidable consequence of attempting such analyses without location information on each tree.

While the effects of these and other limitations are likely to alter CWS in opposing directions, since the magnitude of such effects are currently unknown, it is impossible to say on the basis of current knowledge if the effects cancel one another or if one dominates, with consequent changes to the CWS reported here. What is clear from the above findings is that small to intermediate-scale disturbances can begin to be linked in a mechanistic fashion to meteorological drivers.

Future research

The findings reported here illustrate the need for improved understanding and more data on a number of topics, a few of which we highlight here. Perhaps most obviously, better estimates of CWS for floristically and structurally diverse tropical forests will be facilitated by flexible and reliable estimators of tree allometry and crown architecture, and especially how such estimates vary with tree density and spacing. While this study had the advantage of detailed crown measurements of each individual tree, such data are a luxury that will not often be available, and crown characteristics will typically need to be predicted from easily obtained measures of diameter and perhaps height. Equally important will be efforts to improve knowledge of drag coefficients, which are currently known for only a few temperate broadleaf species, as well as modulus of rupture measurements across a broader range of tropical species. Future dynamic CWS estimates, whether in temperate, boreal or tropical forests, would benefit from improved knowledge of changes in wind characteristics as trees progressively fail. And for species-rich tropical forests, although the sheer number of taxa likely precludes obtaining species-specific parameters on every species, examination of phylogenetic correlations within and among genera and families may allow using either characteristics of representative species, or genus- or family-level parameters of architecture, allometry and stability in future CWS estimates.

A final potential goal for future work relates to our suggestion above that for at least a few tropical trees, increasing crown width may occur during inter-storm intervals such that root and trunk strength cannot keep pace to maintain constant stability. It is well established that trees typically acclimate and adjust morphology to accommodate their local wind environment ([Gardiner et al., 2016](#)). For trunk strength, this idea could be tested easily with crown and trunk measurements followed

by estimation of critical turning moment for trunk breakage. CWS could be calculated for those trees (for trunk breakage) at one time point, and then the trees resampled several years later and similar calculations repeated to see if CWS decreases over time. Analogous calculations for uprooting would require further winching studies.

Conflict of interest statement

None declared.

Funding

The winching study reported in [Ribeiro et al. \(2016\)](#) was funded by the Brazilian Council for Scientific and Technological Development (CNPq) within the projects Succession After Windthrows (SAWI) (Chamada Universal MCTI/No14/2012, Proc. 473357/2012-7), INCT – Madeiras da Amazonia and the Next Generation Ecosystem Experiment (NGEE) Tropics at Lawrence Berkeley National Laboratory, and also supported by the Max-Planck-Institute for Biogeochemistry within the Tree Assimilation and Carbon Allocation Physiology Experiment (TACAPE).

References

- Achim, A., Ruel, J.-C., Gardiner, B.A., Laflamme, G. and Meunier, S. 2005 Modeling the vulnerability of balsam fir forests to wind damage. *Forest Ecol. Manag.* **204**, 35–50. DOI:10.1016/j.foreco.2004.07.072.
- Albini, F.A. and Baughman, R.G. 1979 Estimating windspeeds for predicting wildland fire behavior. USDA Forest Service Research Paper INT-221 (USA).
- Ancelin, P., Courbaud, B. and Fourcaud, T. 2004 Development of an individual tree-based mechanical model to predict wind damage within forest stands. *Forest Ecol. Manag.* **203**, 101–121. DOI:10.1016/j.foreco.2004.07.067.
- Andrade, E.A. and Higuchi, N. 2009 Productivity of four Terra Firme tree species of Central Amazonia. *Acta Amazon.* **39**, 105–112.
- Araujo, B.F., Nelson, B.W., Seles, C.H.S. and Chambers, J.Q. 2017 Regional distribution of large blowdown patches across Amazonia in 2005 caused by a single convective squall line. *Geophys. Res. Lett.* **44**, 7793–7798. DOI:10.1002/2017GL073564.
- Bonnesoeur, V., Fournier, M., Bock, J., Badeau, V., Fortin, M. and Colin, F. 2013 Improving statistical windthrow modeling of 2 *Fagus sylvatica* stand structures through mechanical analysis. *Forest Ecol. Manag.* **289**, 535–543. DOI:10.1016/j.foreco.2012.10.001.
- Brokaw, N.V.L. 1985 Gap-phase regeneration in a tropical forest. *Ecology* **66**, 682–687.
- Byrne, K.E. and Mitchell, S.J. 2013 Testing of WindFIRM/ForestGALES_BC: a hybrid-mechanistic model for predicting windthrow in partially harvested stands. *Forestry* **86**, 185–199. DOI:10.1093/forestry/cps077.
- Cannon, J.B., Barrett, M.E. and Peterson, C.J. 2015. The effect of species, size, failure mode, and fire-scarring on tree stability. *Forest Ecol. Manag.* **356**, 196–203. DOI: 10.1016/j.foreco.2015.07.014.
- Carneiro, V.M.C., Lima, A.J.N., Pinto, A.C., Santos, J., Teixeira, L.M. and Higuchi, N. 2005 Floristic composition and structural analysis of terre firme forests in Manaus, Amazonas, Brazil. In *V Congresso Florestal Nacional: A Floresta e as Gentes*. Rui Silva and Fernando Pascoa (eds). Actas das Comunicações–Inventário, Modelação e Gestão, pp. 1–12.
- Chambers, J.Q., Negrón-Juárez, R.I., Marra, D.M., Di Vittorio, A., Tews, J., Roberts, D., et al 2013 The steady-state mosaic of disturbance and succession across an old-growth Central Amazon forest landscape. *Proc. Natl. Acad. Sci. (USA)* **110**, 3949–3954. DOI:10.1073/pnas.1202894110.
- Chudnoff, M. 1984. *Tropical timbers of the world*. USDA Forest Service Agriculture Handbook number 607. Washington, DC. 466 pp.
- Ciftci, C., Arwade, S.R., Kane, B. and Brena, S.F. 2014 Analysis of the probability of failure for open-grown trees during wind storms. *Probabilist. Eng. Mech.* **37**, 41–50. DOI:10.1016/j.probengmech.2014.04.002.
- Cremer, K.W., Borough, C.J., McKinnel, F.H. and Carter, P.R. 1982 Effects of stocking and thinning on wind damage in plantations. *NZ J. Forest Sci.* **12**, 244–268.
- Cucchi, V., Meredieu, C., Stokes, A., de Coligny, F., Suarez, J. and Gardiner, B.A. 2005 Modelling the windthrow risk for simulated forest stands of Maritime pine (*Pinus pinaster* Ait.). *Forest Ecol. Manag.* **213**, 184–196. DOI: 10.1016/j.foreco.2005.03.019.
- Cullen, S. 2005 Trees and wind: a practical consideration of the drag equation velocity exponent for urban tree risk management. *J. Arboric.* **31**, 101–113.
- da Silva, R.P., dos Santos, J., Tribuzy, E.S., Chambers, J.Q., Nakamura, S. and Higuchi, N. 2002 Diameter increment and growth patterns for individual trees growing in Central Amazon, Brazil. *Forest Ecol. Manag.* **166**, 295–301. DOI:10.1016/S0378-1127(01)00678-8.
- de Santana, R.A.S., Dias-Júnior, C.Q., do Vale, R.S., Tóta, J. and Fitzjarrald, D.R. 2017 Observing and modeling the vertical wind profile at multiple sites in and above the Amazon rain forest canopy. *Adv. Meteorol.* **2017**, article 5436157.
- Denslow, J.S. 1980 Gap partitioning among tropical rainforest trees. *Biotropica* **12**, 47–55.
- Dunham, R.A. and Cameron, A.D. 2000 Crown, stem and wood properties of wind-damaged and undamaged Sitka spruce. *Forest Ecol. Manag.* **135**, 73–81. DOI:10.1016/S0378-1127(00)00299-1.
- Dupont, S., Pivato, D. and Brunet, Y. 2015 Wind damage propagation in forests. *Agric. For. Meteorol.* **214–215**, 243–251. DOI:10.1016/j.agrformet.2015.07.010.
- Ferraz, J., Oht, S. and Salles, P.C. 1998 Distribuição dos solos ao longo de dois transectos em floresta primária ao norte de Manaus (AM). In *Pesquisas Florestais para a Conservação da Floresta e Reabilitação de Áreas Degradadas da Amazônia*. Higuchi N., Campos M.A.A., Sampaio P.T. B. and Santos J. (eds). INPA, pp. 111–143.
- Filho, A.D.M., Dallarosa, R.G. and Pachêco, V.B. 2005 Radiação solar e distribuição vertical de área foliar em floresta – Reserva Biológica do Cuieiras ZF2, Manaus. *Acta Amazon.* **35**, 427–436.
- Foster, D.R. 1988 Species and stand response to catastrophic wind in central New England, USA. *J. Ecol.* **76**, 135–151.
- Gardiner, B., Peltola, H. and Kellomaki, S. 2000 Comparison of two models for predicting the critical wind speeds required to damage coniferous trees. *Ecol. Modell.* **129**, 1–23. DOI:10.1016/S0304-3800(00)00220-9.
- Gardiner, B., Byrne, K., Hale, S., Kamimura, K., Mitchell, S.J., Peltola, H., et al 2008 A review of mechanistic modelling of wind damage risk to forests. *Forestry* **81**, 447–463. DOI:10.1093/forestry/cpn022.
- Gardiner, B., Berry, P. and Moulia, B. 2016 Review: wind impacts on plant growth, mechanics and damage. *Plant Sci.* **245**, 94–118. DOI:10.1016/j.plantsci.2016.01.006.
- Garstang, M., White, S., Shugart, H.H. and Halverson, J. 1998 Convective cloud downdrafts as the cause of large blowdowns in the Amazon rainforest. *Meteorol. Atmos. Phys.* **67**, 199–212. DOI:10.1007/BF01277510.
- Hale, S.E., Gardiner, B., Wellpott, A., Nicoll, B.C. and Achim, A. 2012 Wind loading of trees: influence of tree size and competition. *Eur. J. For. Res.* **131**, 203–217. DOI:10.1007/s10342-010-0448-2.
- Hale, S.E., Gardiner, B., Peace, A., Nicoll, B., Taylor, P. and Pizzirani, S. 2015 Comparison and validation of three versions of a forest wind risk

- model. *Environ. Model. Softw.* **68**, 27–41. DOI:10.1016/j.envsoft.2015.01.016.
- Hallé, F., Oldeman, R.A.A. and Tomlinson, P.B. 1978 *Tropical trees and forests: An architectural analysis*. Springer.
- Hart, E., Sim, K., Kamimura, K., Meredieu, C., Guyon, D. and Gardiner, B. 2019 Use of machine learning techniques to model wind damage to forests. *Agric. For. Meteorol.* **265**, 16–29. DOI:10.1016/j.agrformet.2018.10.022.
- Higuchi, N., Dos Santos, J., Ribeiro, R.J., Freitas, J.V., Vieira, G. and Cornic, A. 1997 Crescimento e Incremento de uma Floresta Amazônica de Terra-Firme Manejada Experimentalmente. In *Biomassa de Nutrientes Florestais*. N. Higuchi (ed). INPA, pp. 89–132.
- Higuchi, N., Chambers, J.Q., Santos, J., Ribeiro, R.J., Pinto, A.C., Silva, R.P., et al 2004 Carbon balance and dynamics of primary vegetation in the central Amazon. *Floresta* **34**, 295–304.
- Johnson, E. and Miyanishi, K. 2007 Introduction. In *Plant Disturbance Ecology: The Process and the Response*. Johnson E.A. and Miyanishi K. (eds). Academic Press, pp. 15–25.
- Kamimura, K., Gardiner, B., Kato, A., Hiroshima, T. and Shiraishi, N. 2008 Developing a decision support approach to reduce wind damage risk – a case study on sugi (*Cryptomeria japonica* (L.f.) D.Don) forests in Japan. *Forestry* **81**, 429–445. DOI:10.1093/forestry/cpn029.
- Kamimura, K., Gardiner, B.A., Dupont, S., Guyon, D. and Meredieu, C. 2016 Mechanistic and statistical approaches to predicting wind damage to individual maritime pine (*Pinus pinaster*) trees in forests. *Can. J. For. Res.* **46**, 88–100. DOI:10.1139/cjfr-2015-0237.
- Kamimura, K., Gardiner, B.A. and Koga, S. 2017 Observations and predictions of wind damage to *Larix kaempferi* trees following thinning at an early growth stage. *Forestry* **90**, 530–540. DOI:10.1093/forestry/cpx006.
- Kane, B., Pavlis, M., Harris, J.R. and Seiler, J.R. 2008 Crown reconfiguration and trunk stress in deciduous trees. *Can. J. For. Res.* **38**, 1275–1289. Doi:10.1139/X07-225.
- Kenk, G. and Guehne, S. 2001 Management of transformation in central Europe. *Forest Ecol. Manag.* **151**, 107–119.
- Kozak, A., Munro, D.D. and Smith, J.H.G. 1969 Taper functions and their application in forest inventory. *Forest. Chron.* **45**, 278–283.
- Lima, A.J.N., Teixeira, L.M., Carneiro, V.M.C., Santos, J. and Higuchi, N. 2007 Biomass stock and structural analysis of a secondary forest in Manaus (AM) region, ten years after clear cutting followed by fire. *Acta Amazon.* **37**, 49–54.
- Locatelli, T., Gardiner, B., Tarantola, S., Nicoll, B., Bonnefond, J.M., Garrigou, D., et al 2016 Modelling wind risk to *Eucalyptus globulus* (Labill.) stands. *Forest Ecol. Manag.* **365**, 159–173. DOI:10.1016/j.foreco.2015.12.035.
- Locatelli, T., Tarantola, S., Gardiner, B. and Patenaude, G. 2017 Variance-based sensitivity analysis of a wind risk model – model behavior and lessons for forest modelling. *Environ. Model. Softw.* **87**, 84–109. DOI:10.1016/j.envsoft.2016.10.010.
- Luizao, R.C.C., Luizao, F.J., Paiva, R.Q., Monteiro, T.F., Sousa, L.S. and Kruijt, B. 2004 Variation of carbon and nitrogen cycling processes along a topographic gradient in a central Amazonian forest. *Glob. Change Biol.* **10**, 592–600. DOI:10.1111/j.1529-8817.2003.00757.x.
- Magnabosco Marra, D., Chambers, J.Q., Higuchi, N., Trumbore, S.E., Ribeiro, G.H.P.M., dos Santos, J., et al 2014 Large-scale wind disturbances promote tree diversity in a Central Amazon forest. *PLoS One* **9** (8), e103711. DOI:10.1371/journal.pone.0103711.
- Magnabosco Marra, D., Trumbore, S.E., Higuchi, N., Ribeiro, G.H.P.M., Negrón-Juárez, R.I., Holzwarth, F., et al 2018 Windthrows control biomass patterns and functional composition of Amazon forests. *Global Change Biol.* **24**, 5867–5881. DOI:10.1111/gcb.14457.
- Martin, A.J. 1981 Taper and volume equations for selected Appalachian hardwood species. USDA Forest Service, Research Paper NE-490. 26 pp.
- Mason, W.L. 2002 Are irregular stands more windfirm? *Forestry* **75**, 347–355.
- Mitchell, R.J., Hiers, J.K., O'Brien, J.J. and Starr, G. 2009 Ecological forestry in the Southeast: understanding the ecology of fuels. *J. Forestry* **107**, 391–397.
- Mitchell, S.J. 2013 Wind as a natural disturbance agent in forests: a synthesis. *Forestry* **86**, 147–157. DOI:10.1093/forestry/cps058.
- Mitchell, S.J. and Ruel, J.-C. 2015 Modeling windthrow at stand and landscape scales. In *Simulation Modeling of Forest Landscape Disturbances*. Perera A.H., Sturtevant B.R. and Buse L.J. (eds). Springer, pp. 17–43.
- Nelson, B.W., Kapos, V., Adams, J.B., Oliveira, W.J. and Braun, G.P. 1994 Forest disturbance by large blowdowns in the Brazilian Amazon. *Ecology* **75**, 853–858.
- Negrón-Juárez, R.I., Chambers, J.Q., Guimaraes, G., Zeng, H., Raupp, C.F.M., Marra, D.M., et al 2010 Widespread Amazon forest tree mortality from a single cross-basin squall line event. *Geophys. Res. Lett.* **37**, L16701. doi:10.1029/2010GL943733.
- Negrón-Juárez, R.I., Jenkins, H.S., Raupp, C.F.M., Riley, W.J., Kueppers, L.M., Marra, D.M., et al 2017 Windthrow variability in Central Amazonia. *Atmosphere* **8**, 28. doi:10.3390/atmos8020028.
- Negrón-Juárez, R.I., Holm, J.A., Marra, D.M., Rifai, S.W., Riley, W.J., Chambers, J.Q., et al 2018 Vulnerability of Amazon forests to storm-driven tree mortality. *Environ. Res. Lett.* **13**, article 054021. doi:10.1088/1748-9326/aabe9f.
- Nicoll, B.C., Gardiner, B.A., Rayner, B. and Peace, A.J. 2006 Anchorage of coniferous trees in relation to species, soil type, and rooting depth. *Can. J. For. Res.* **36**, 1871–1883. DOI:10.1139/X06-072.
- Peltola, H. 2006 Mechanical stability of trees under static loads. *Am. J. Bot.* **93**, 1501–1511. DOI:10.3732/ajb.93.10.1501.
- Peltola, H. and Kellomaki, S. 1993 A mechanistic model for calculating windthrow and stem breakage of Scots pines at stand edge. *Silva Fenn.* **27**, 99–111.
- Peltola, H., Kellomaki, S., Vaisanen, H. and Ikonen, V.-P. 1999 A mechanistic model for assessing the risk of wind and snow damage to single trees and stands of Scots pine, Norway spruce, and birch. *Can. J. For. Res.* **29**, 647–661. DOI:10.1139/cjfr-29-6-647.
- Quine, C.P. and Gardiner, B.A. 2007 Understanding how the interaction of wind and trees results in windthrow, stem breakage and canopy gap formation. In *Plant Disturbance Ecology: The Process and the Response*. Johnson E.A. and Miyanishi K. (eds). Academic Press, pp. 103–155.
- Renno, C.D., Nobre, A.D., Cuartas, L.A., Soares, J.V., Hodnett, M.G., Tomasella, J., et al 2008 HAND, a new terrain descriptor using SRTM-DEM: Mapping terra-firme rainforest environments in Amazonia. *Remote Sens. Environ.* **112**, 3469–3481.
- Ribeiro, J.E.L.S., Hopkins, M.J.G., Vicentini, A., Sothers, C.A., Costa, M.A.S., de Brito, J.M., et al 1999 Flora da Reserva Ducke. Guia de identificação das plantas vasculares de uma floresta de terra-firme na Amazonia Central. INPA/DIFD.
- Ribeiro, G.H.P.M., Chambers, J.Q., Peterson, C.J., Trumbore, S.E., Magnabosco Marra, D., Wirth, C., et al 2016 Mechanical vulnerability and resistance to snapping and uprooting for Central Amazon tree species. *Forest Ecol. Manag.* **380**, 1–10. DOI:10.1016/j.foreco.2016.08.039.
- Rifai, S.W., Urquiza Muñoz, J.D., Negrón-Juárez, R.I., Ramirez Arévalo, F.R., Tello-Espinoza, R., Vanderwel, M.C., et al 2016 Landscape-scale consequences of differential tree mortality from catastrophic wind disturbance in the Amazon. *Ecol. Appl.* **26**, 2225–2237. DOI:10.1002/eap.1368.

- Ruel, J.-C., Quine, C.P., Meunier, S. and Suarez, J. 2000 Estimating wind-throw risk in balsam fir stands with the ForestGALES model. *Forest Chron.* **76**, 329–337.
- Saito, S., Sakai, T., Nakamura, S. and Higuchi, N. 2003 Three types of seedling establishments of tree species in an Amazonian terra-firme forest. In *Projeto Jacaranda Fase II: Pesquisas florestais na Amazonia*. Higuchi N. (ed). INPE, pp. 33–41.
- Schelhaas, M.J., Kramer, K., Peltola, H., van der Wef, D.C. and Wijdeven, S.M.J. 2007 Introducing tree interactions in wind damage simulation. *Ecol. Model.* **207**, 197–209. DOI:10.1016/j.ecolmodel.2007.04.025.
- Seidl, R., Rammer, W. and Blennow, K. 2014 Simulating wind disturbance impacts on forest landscapes: tree-level heterogeneity matters. *Environ. Model. Softw.* **51**, 1–11. DOI:10.1016/j.envsoft.2013.09.018.
- Silverio, D.V., Brando, P.M., Bustamante, M.M.C., Putz, F.E., Marra, D.M., Levick, S.R., et al 2019 Fire, fragmentation, and windstorms: a recipe for tropical forest degradation. *J. Ecol.* **107**, 656–667. DOI:10.1111/1365-2745.13076.
- Sombroek, W. 2001 Spatial and temporal patterns of Amazon rainfall – consequences for the planning of agricultural occupation and the protection of primary forests. *Ambio* **30**, 388–396.
- Tomlinson, P.B. 1983 Tree architecture. *Am. Sci.* **71**, 141–149.
- Tóta, J., Fitzjarrald, D.R. and Da Silva Dias, M.A.F. 2012 Amazon rainforest exchange of carbon and subcanopy air flow: Manaus LBA Site – a complex terrain condition. *Sci. World J.* **2012**, article 165067.
- Vieira, S., de Camargo, P.B., Selhorst, D., da Silva, R., Hutya, L., Chambers, J.Q., et al 2004 Forest structure and carbon dynamics in Amazonian tropical rain forests. *Oecologia* **140**, 468–479. DOI:10.1007/s00442-004-1598-z.
- Vollsinger, S., Mitchell, S.J., Byrne, K.E., Novak, M.D. and Rudnicki, M. 2005 Wind tunnel measurements of crown streamlining and drag relationships for several hardwood species. *Can. J. For. Res.* **35**, 1238–1249. DOI:10.1139/x05-051.
- Whitmore, T.C. 1989 Canopy gaps and the two major groups of forest trees. *Ecology* **70**, 536–538.